Geophys. J. Int. (1998) **132,** 383–400

Structure of the Jan Mayen microcontinent and implications for its evolution

Shuichi Kodaira,[1,*] Rolf Mjelde,[1] Karl Gunnarsson, [2] Hajime Shiobara[3] and Hideki Shimamura[3]

[1] *Institute of Solid Earth Physics, University of Bergen, Allégt.* 41, 5007 *Bergen, Norway*
[2] *National Energy Authority, Grensasvergu* 9, 108, *Reykjavik, Iceland*
[3] *Laboratory for Ocean Bottom Seismology, Hokkaido University,* N10W8 *Kita-ku Sapporo* 060, *Japan*

Accepted 1997 September 19. Received 1997 September 9; in original form 1996 May 21

SUMMARY

An extensive seismic survey using ocean-bottom seismographs (OBS) was performed in the area across the Jan Mayen Basin, North Atlantic, from the Jan Mayen Ridge to the Iceland Plateau. The Jan Mayen Ridge and surrounding area are considered to be a fragment of a continent which was separated from Greenland just prior to magnetic anomaly 6. This study presents the crustal structure of the Jan Mayen microcontinent and the ocean/continent transition to the west of the Jan Mayen Ridge. The crustal structures from the centre of the Jan Mayen Ridge to the Jan Mayen Basin are characterized by a deep sedimentary basin, a thin basaltic layer within the sedimentary section and extreme thinning of the continental crust towards the Iceland Plateau. The OBS data indicate that a continental upper crust ($V_p = 5.8$–6.1 km s^{-1}) and lower crust ($V_p = 6.7$–6.8 km s^{-1}) underlie the deep sedimentary basin. The thickness of the continental lower crust varies significantly from 12 km beneath the Jan Mayen Ridge to almost zero thickness beneath the northwestern part of the Jan Mayen Basin. An ocean/continent transition zone is found at the western edge of the Jan Mayen Basin. Within the 10 km wide transition zone, crustal velocities increase towards the Iceland Plateau, and approach the velocities of the oceanic crust obtained at the Iceland Plateau, that is 3.8–5.1 km s^{-1} (oceanic layer 2A), 5.9–6.5 km s^{-1} (oceanic layer 2B) and 6.8–7.3 km s^{-1} (oceanic layer 3). The crustal model indicates very thin oceanic crust (5 km) immediately oceanwards of the ocean/continent transition zone. Beneath the Iceland Plateau, the oceanic crust is thicker (9 km) than the typical thickness of normal oceanic crust. This might imply that the oceanic crust at the Iceland Plateau has been generated by asthenospheric material slightly hotter than normal. From the crustal structure obtained by the present study, it is proposed that the western part of the Jan Mayen Ridge may be referred to as a non-volcanic continental margin, generated by a long duration of rifting. Even if the asthenospheric material upwelling along the margin were hotter than normal, only small amounts of magmatic intrusions and extrusions would have been generated because of significant conductive cooling under the long duration of rifting.

Key words: continental margin, crustal structure, Jan Mayen Ridge, rift, seismic refraction.

INTRODUCTION

The Jan Mayen Ridge is a submarine structure extending southward from Jan Mayen Island in the North Atlantic (Fig. 1) trending in a N–S direction (Fig. 2). At about 69°N, the trend of the ridge changes slightly to NE–SW. The water depth at the crest of the ridge increases from north to south, with an average depth of less than 1000 m. The *c.* 50 km wide Jan Mayen Basin is located to the west of the ridge. In this basin, the seafloor is smooth with water depths greater than 2000 m (Fig. 2). The Iceland Plateau, which is believed to consist of oceanic crust (Vogt, Johnson & Kristjansson 1980),

* Now at: Deep Sea Research Department, Japan Marine Science & Technology Center, Natsushima 2–15, Yokosuka, 237, Japan. E-mail: kodaira@jamstec.go.jp

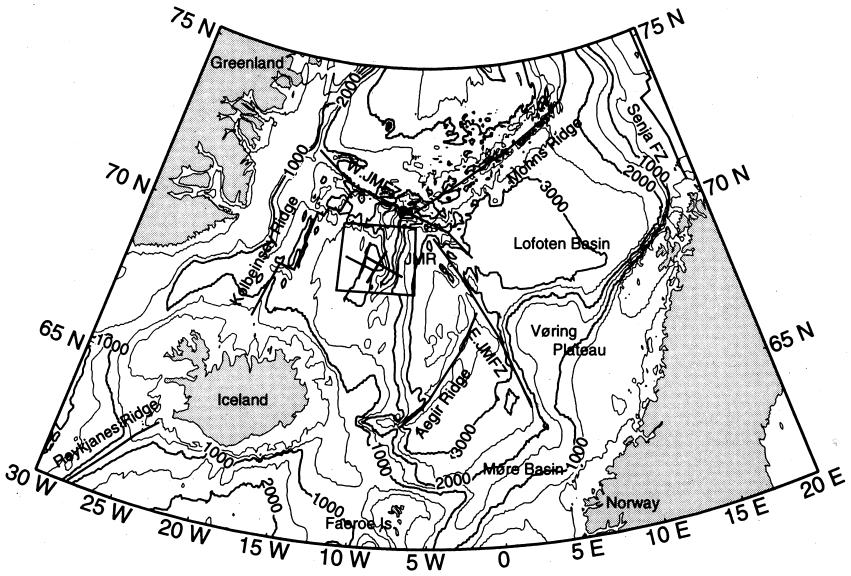

Figure 1. Regional physiography and structural features in the Norwegian–Greenland Sea. The detailed map of the framed area is shown in Fig. 2. W.JMFZ: West Jan Mayen Fracture Zone; E.JMFZ: East Jan Mayen Fracture Zone; JMR; Jan Mayen Ridge.

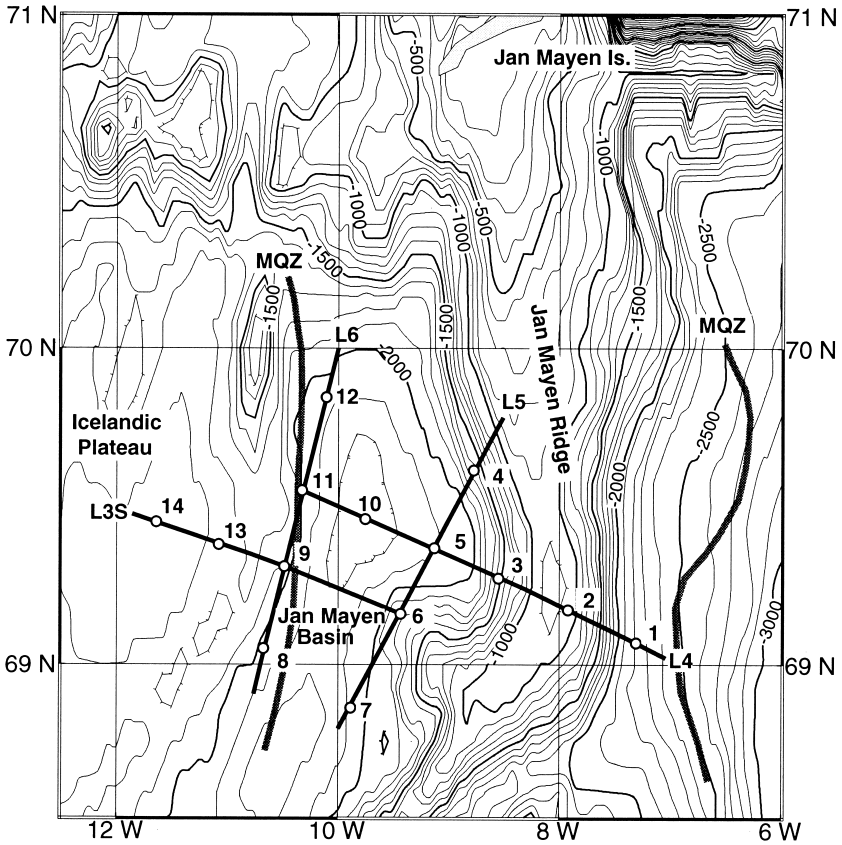

Figure 2. Survey area with OBS profiles. L3S, L4, L5 and L6 represent the OBS profiles, and numbers 1–14 indicate the OBS positions. MQZ: edges of a magnetic quiet zone compiled by Olafsson (1983).

is situated to the west of the Jan Mayen Basin. To the east of the Jan Mayen Ridge, the water depth increases gradually towards the deep Norway Basin.

During the last three decades, the Jan Mayen Ridge and surrounding areas have been investigated using several geophysical methods, including deep-sea drilling (Talwani & Udintsev 1976; Talwani *et al.* 1978; Udintsev & Kharin 1978), gravity studies (Talwani & Grønlie 1976; Grønlie, Chapman & Talwani 1979; Grønlie & Talwani 1982), magnetic studies (Talwani & Eldholm 1977; Grønlie *et al.* 1979; Navrestad & Jørgensen 1979; Vogt *et al.* 1980), seismic refraction studies (Eldholm & Windisch 1974; Talwani & Eldholm 1977; Garde

1978; Stoffa & Buhl 1979; Sundvor *et al.* 1979; Myhre & Eldholm 1981; Johansen *et al.* 1988; Olafsson & Gunnarsson 1989) and seismic reflection profiling (Gairand *et al.* 1978; Navrestad & Jørgensen 1979; Olafsson 1983; Skogseid & Eldholm 1987; Gudlaugsson *et al.* 1988). A magnetic study (Talwani & Eldholm 1977) showed a magnetically quiet zone between the eastern flank of the Jan Mayen Ridge and the western edge of the Jan Mayen Basin. Myhre (1984) examined the shallow crustal velocity structure around the Jan Mayen Ridge (down to 6 km depth), and concluded that the velocity stratification of the Jan Mayen Ridge is similar to that of the Norwegian and East Greenland continental margins landwards of the ocean/continent boundary. Multichannel reflection data clarified shallow sedimentary structures and resolved an Early Tertiary basaltic layer at the eastern flank of the ridge. These structures were interpreted as representing structures conjugate to those present along the Norwegian continental margin (Skogseid & Eldholm 1987). From the top of the ridge to the western flank, multichannel reflection data showed large rotated fault blocks (Skogseid & Eldholm 1987). Based on those results, most investigators support the hypothesis that the Jan Mayen Ridge is a continental fragment (a 'microcontinent'), which was originally part of the Greenland continental margin (e.g. Myhre, Eldholm & Sundvor 1984).

Several crustal studies around the North Atlantic continental margin have defined structures across the ocean/continent transition that are important in understanding continental rifting and oceanic spreading processes (White *et al.* 1987; Mutter, Buck & Zehnder 1988; Fowler *et al.* 1989; Olafsson *et al.* 1992; Mjelde *et al.* 1992; Goldschmidt-Rokita *et al.* 1994; Kodaira *et al.* 1995). Moreover, widespread influence of the Iceland hot spot throughout much of the North Atlantic has been suggested (McKenzie & Bickle 1988) based on the huge volumes of high-velocity ($V_p > 7.3$ km s^{-1}) material in the lower crust and the ubiquitous flood basalts found landwards of the ocean/continent transition zones (White & McKenzie 1989).

The shallow to deep crustal structure across the Jan Mayen Ridge is thus important in understanding rifting and magmatic processes in the North Atlantic and the formation of the Jan Mayen 'microcontinent' in this broader setting. Due to the presence of basaltic layers at the eastern flank of the ridge and in the Jan Mayen Basin, as well as thick sediments beneath the western flank of the ridge, the deep crustal structure around the Jan Mayen Ridge has not been determined either by previous multichannel reflection surveys (Skogseid & Eldholm 1987) or sonobuoy refraction or by ESP studies (Myhre 1984; Olafsson & Gunnarsson 1989). The purpose of the present study is to map the whole crustal structure from the eastern flank of the Jan Mayen Ridge to the Iceland Plateau, and to investigate the process of formation of the Jan Mayen Ridge as a submarine 'microcontinent'.

TECTONIC SETTING

The seafloor spreading process between the West–East Jan Mayen Fracture Zone and the Faeroe–Iceland aseismic ridge is not as simple as that along the Mohns Ridge, to the north of the Kolbeinsey Ridge (Fig. 1). Along the Mohns Ridge, oceanic crust has been generated symmetrically since oceanic spreading started. It is believed, however, that oceanic spreading between the West–East Jan Mayen Ridge and the Faeroe–Iceland aseismic ridge was associated with major westward shifts of the spreading axis (Eldholm *et al.* 1990; Talwani & Eldholm 1977).

Eldholm *et al.* (1990) described the tectonic history of this area as follows: just prior to magnetic anomaly 23, the oceanic spreading started along and to the west of the Faeroe–Shetland Escarpment. The ocean/continent transitional structure at the eastern flank of the Jan Mayen Ridge was formed during this episode. Oceanic spreading progressed along the Aegir Ridge during magnetic anomalies 23–13. The rift axis then migrated to the Greenland margin, and a part of the Greenland margin, which is the present-day Jan Mayen Ridge, was completely separated at magnetic anomalies 7–6. The ocean/continent structure to the west of the Jan Mayen Ridge, which is within the survey area of this study, is considered to have been generated during this episode.

There is no general agreement regarding the tectonic history of the Iceland Plateau between magnetic anomalies 7 and 5. Grønlie *et al.* (1979) proposed an extinct spreading axis to the west of the Jan Mayen Ridge where the oceanic spreading continued until just prior to magnetic anomaly 5, before the spreading axis jumped to the present-day Kolbeinsey Ridge. Vogt *et al.* (1980), however, argued against the existence of an extinct axis. They proposed continuous spreading along the Kolbeinsey Ridge after magnetic anomaly 7, with an increase in full spreading rate from 15 to 20 mm yr^{-1} at magnetic anomaly 5. As magnetic anomaly 5 and younger anomalies are well developed on both flanks of the Kolbeinsey Ridge (Vogt *et al.* 1980), it is generally accepted that oceanic spreading has progressed along the present-day spreading ridge (the Kolbeinsey Ridge) since magnetic anomaly 5 (Eldholm *et al.* 1990).

DATA ACQUISITION AND MODELLING PROCEDURE

In the spring of 1995, the universities of Bergen (Norway) and Hokkaido (Japan), in cooperation with the National Energy Authority (Iceland), performed an extensive geophysical experiment in the area between the Jan Mayen Ridge and the Kolbeinsey Ridge (Fig. 1). Data from ocean-bottom seismographs (OBS), described in the present study, were acquired as a part of this experiment. The details of the whole experiment are described by Mjelde, Kodaira & Shimamura (1995).

Locations of the OBS profiles used in this study are shown in Fig. 2. Two profiles (Fig. 2) from the Iceland Plateau to the Jan Mayen Ridge (L3S and L4) were acquired to determine crustal structure from the oceanic crust to the presumed continental crust. The lengths of L3S and L4 are about 100 and 140 km, respectively. In addition, two profiles (125 km) were acquired along the eastern and western edge of the Jan Mayen Basin (L5 and L6), where the presence of the ocean/continent transition zone had previously been suggested (Vogt *et al.* 1980). A total of 14 OBSs were deployed along the four profiles, and single-channel reflection data were also acquired along all profiles. Parts of L4 and L5 were situated on multichannel reflection profiles previously acquired by the Norwegian Petroleum Directorate.

A tuned air-gun array consisting of one Bolt 1500 C air-gun and five airguns on a string with a total volume of 2036 in^3 (33.4 l) were fired every minute at about 125 m intervals along L4, L5 and L6. Along L3S, a slightly smaller-volume tuned

air-gun array (1996 $in^3 = 32.7$ l) was used, but the shot interval was the same as along the other profiles. The OBSs used have three-component gimbal-mounted geophones. The instruments record continuously for 14 days within the 1–30 Hz frequency range (−3 dB) (Kanazawa 1986; Shimamura 1988; Kanazawa & Shiobara 1994). As described in previous OBS studies of the Norwegian margin, only a bandpass filter was applied due to the high quality of the OBS data (Mjelde *et al.* 1992; Kodaira *et al.* 1995; Mjelde *et al.* 1997), and all OBS data presented in this paper have been 5–20 Hz bandpass filtered (Fig. 3).

Crustal models were obtained using the 2-D traveltime inversion method of Zelt & Smith (1992) together with forward kinematic and dynamic modelling (Zelt & Ellis 1988). Prominent interfaces recognized in the single-channel and multichannel reflection data were included in starting models for the traveltime inversion. This inversion is performed in a layer by layer fashion where the parameters of successively deeper layers are determined whilst the parameters defining the shallower layers remain fixed. First arrivals and reflection traveltimes observed on the OBSs were digitized with estimated uncertainties depending on signal-to-noise ratios (0.05–0.2 s). Both the velocities (top and bottom in each layer) and the geometries of the crustal models were derived using these observed traveltimes. In order to obtain good resolution in the deeper part of the lower crust, the velocities of the lower crust, geometry of the top of the lower crust and Moho were inverted simultaneously using the lower-crustal refraction and Moho reflection phases (*PmP*).

One advantage of this inversion procedure is that it allows velocity and interface nodes to be specified independently, allowing the reliability of the final model to be estimated. The resolution value represents the diagonal elements of the resolution matrix and indicates relative ray coverage at the nodes (Zelt & Smith 1992). Node points with resolution value greater than 0.5 are considered to be well resolved. Even though resolution values are not directly related to absolute parameter uncertainties (Zelt & Smith 1992), we note that higher resolution (that is higher ray coverage) is usually associated with lower uncertainty. Zelt & Smith (1992) proposed a method to estimate a parameter's absolute uncertainty. However, they suggested that it might not be a practical way to estimate all model uncertainties, since applying their proposed error analysis to all velocity and boundary nodes could take longer than the time required to obtain the final model. We have therefore, tested only a few representative velocity nodes. As results of those tests we found that velocity parameters with resolutions of greater than 0.5 cannot be varied by more than 0.1 km s^{-1} and yet still fit the calculated traveltimes to the observed data within the estimated uncertainties. Final models were constrained by amplitude modelling, which is calculated using zero-order asymptotic ray theory (Červený, Molokkov & Pšenčík 1977). However, due to large uncertainties in such amplitude modelling (Mjelde *et al.* 1997), we considered only the overall character of the amplitude variations with offset by visual comparison (Fig. 3). We paid special attention to the two following features, which are not considered during the traveltime inversion: the range of distances over which each refraction phase was observed; and the location of the critical point of the reflection phases. These features control the velocity gradient in each layer and the velocity contrast between layers, respectively.

CRUSTAL MODELS AND DISCUSSION

Eastern flank of the Jan Mayen Ridge

Fig. 4 shows the crustal model of L4, which crosses the Jan Mayen Ridge and extends to the Jan Mayen Basin. The calculated traveltimes from this model are shown in Fig. 5 with the observed traveltimes. Between OBS1 and OBS5, the geometry of the shallow structures was obtained from the previously obtained (depth-converted) multichannel reflection data down to the top of the 4.0 km s^{-1} layer on the western flank of the ridge, and the top of the flood basalts on the eastern flank.

At the eastern flank of the ridge, previous reflection studies indicated the presence of flood basalts beneath the Cenozoic sediments (Skogseid & Eldholm 1987). The OBS data resolved the velocities of these layers as, in order to obtain the best traveltime fit, velocities of 2.2–2.4 km s^{-1} and 4.6–4.8 km s^{-1} are inferred in the Cenozoic sediments and flood basalts, respectively. Beneath the flood basalts, the model indicates the presence of a thin layer of (presumed Mesozoic) sediments, but as shown in Figs 5 and 6(b), no observed refraction phases are obtained from this layer. We therefore assume that these sediments, which are inferred at the western flank of the Jan Mayen Ridge as described below, extend to the eastern flank. This assumption is in agreement with crustal models along the Norwegian continental margin, where OBS studies indicate sediments beneath the flood basalts (Mjelde *et al.* 1992; Mjelde *et al.* 1997).

Underlying the sediments, the model indicates a two-layered crystalline crust ($V_p = 6.0$–6.4 km s^{-1} and 6.7–6.8 km s^{-1}), similar to the velocity structure obtained at the Møre and Vøring margin (mid- to northern Norway) by ESP studies (Mutter *et al.* 1988; Olafsson *et al.* 1992). Moreover, at the Lofoten margin, northern Norway, velocities of 6.0 and 6.8 km s^{-1} were estimated in the continental upper and lower crust, respectively, by OBS studies (Mjelde *et al.* 1992; Mjelde *et al.* 1993). The two layers obtained at the eastern flank of the Jan Mayen Ridge are thus interpreted as continental upper and lower crust. The thickness of the continental upper crust is about 3 km, and the thickness of the continental lower crust decreases from 12 to 8 km towards the southwest. Crustal thickness is greatest slightly eastwards of the ridge centre (Fig. 4). An upper-mantle reflector is revealed by a sharp mantle reflection phase at OBS3. This reflector is observed only beneath the ridge centre at 23 km depth (Fig. 5).

A significant difference from the crustal structure at the Norwegian continental margin is found in the lower crust. At the Norwegian margin, high-velocity underplated material ($V_p > 7.1$ km s^{-1}) beneath the continental lower crust has been interpreted from seismic studies (Mutter *et al.* 1988; Olafsson *et al.* 1992; Mjelde *et al.* 1997). However, the model of L4 does not indicate any evidence of high-velocity material beneath the Jan Mayen Ridge. As shown in Fig. 6(d), it might be possible to construct an acceptable model incorporating high-velocity material in the lower crust at the southeastern end of the profile, since the ray coverage in the lower crust at the southeastern end of the profile is poor. However, we emphasize that any such high-velocity material cannot extend beneath OBS2, since no clear reflection phases are observed between the lower crustal refraction phase and the Moho reflection

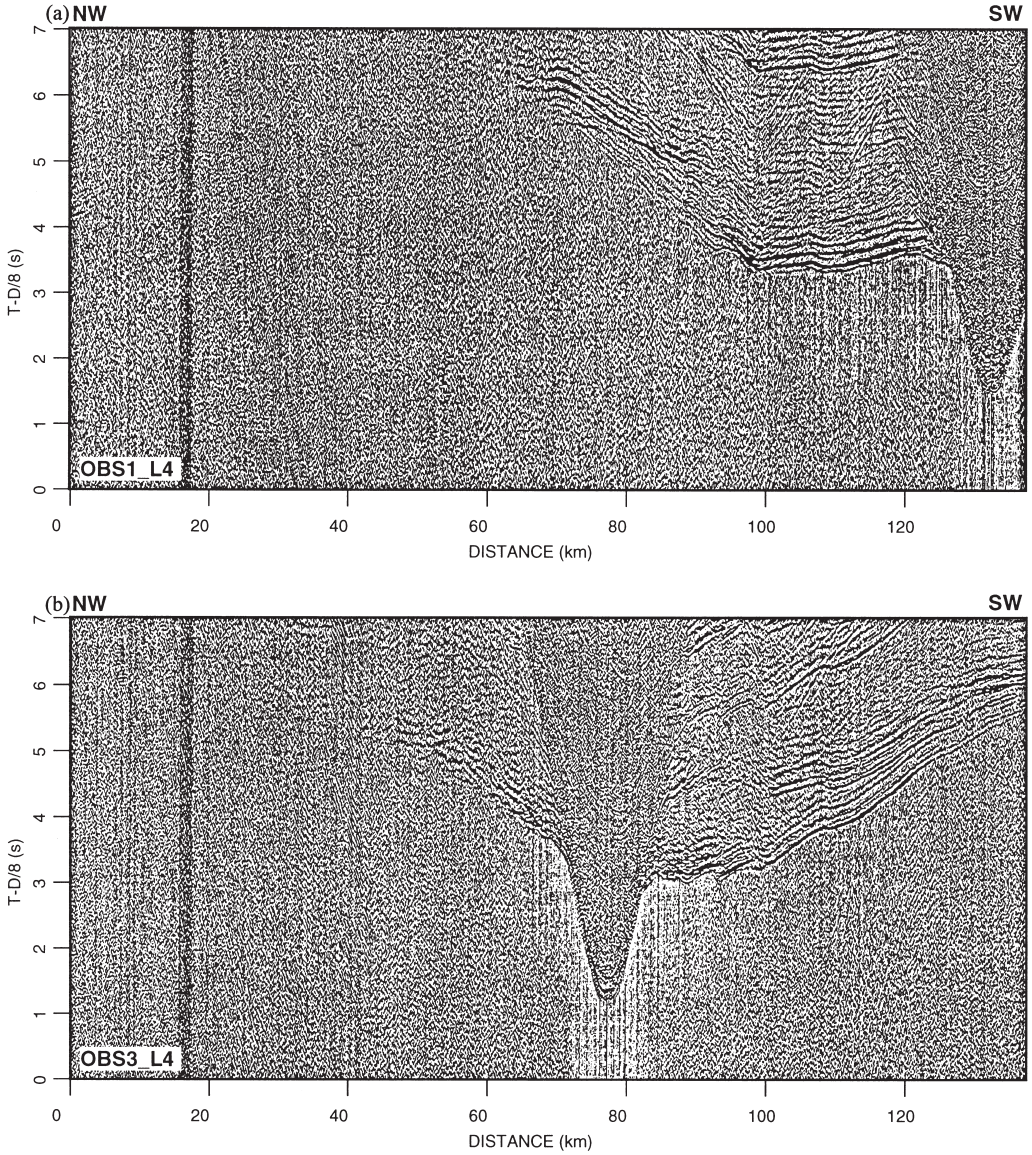

Figure 3. (a) Observed seismic section of the vertical component of OBS1 on L4. 5–20 Hz bandpass filter and 4 s window automatic gain control are applied. The reduction velocity is 8 km s^{-1}. The horizontal axis represents the distance from the northwestern end of L4 (Fig. 2). (b) Observed seismic section of the vertical component of OBS3 on L4. 5–20 Hz bandpass filter and 4 s window automatic gain control are applied. The reduction velocity is 8 km s^{-1}. The horizontal axis represents the distance from the northwestern end of L4 (Fig. 2). (c) Synthetic seismograms of OBS3 on L4 calculated from the crustal model shown in Fig. 4. Direct water-wave arrivals are not included. (d) Observed seismic section of the vertical component of OBS5 on L4. 5–20 Hz bandpass filter and 4 s window automatic gain control are applied. The reduction velocity is 8 km s^{-1}. The horizontal axis represents the distance from the northwestern end of L4 (Fig. 2). (e) Synthetic seismograms of OBS5 on L4 calculated from the crustal model shown in Fig. 4. Direct water-wave arrivals are not included. (f) Observed seismic section of the vertical component of OBS6 on L5. 5–20 Hz bandpass filter and 4 s window automatic gain control are applied. The reduction velocity is 8 km s^{-1}. The horizontal axis represents the distance from the southwestern end of L5 (Fig. 2). (g) Synthetic seismograms of OBS6 on L5 calculated from the crustal model shown in Fig. 7. Direct water-wave arrivals are not included. (h) Observed seismic section of the vertical component of OBS6 on L3S. 5–20 Hz bandpass filter and 4 s window automatic gain control are applied. The reduction velocity is 8 km s^{-1}. The horizontal axis represents the distance from the northwestern end of L3S (Fig. 2). (i) Synthetic seismograms of OBS6 on L3S calculated from the crustal model shown in Fig. 9. Direct water-wave arrivals are not included. (j) Observed seismic section of the vertical component of OBS13 on L3S. 5–20 Hz bandpass filter and 4 s window automatic gain control are applied. The reduction velocity is 8 km s^{-1}. The horizontal axis represents the distance from the northwestern end of L3S (Fig. 2). (k) Observed seismic section of the vertical component of OBS11 on L6. 5–20 Hz bandpass filter and 4 s window automatic gain control are applied. The reduction velocity is 8 km s^{-1}. The horizontal axis represents the distance from the southwestern end of L6 (Fig. 2). (l) Synthetic seismograms of OBS11 on L6 calculated from the crustal model shown in Fig. 12. Direct water-wave arrivals are not included.

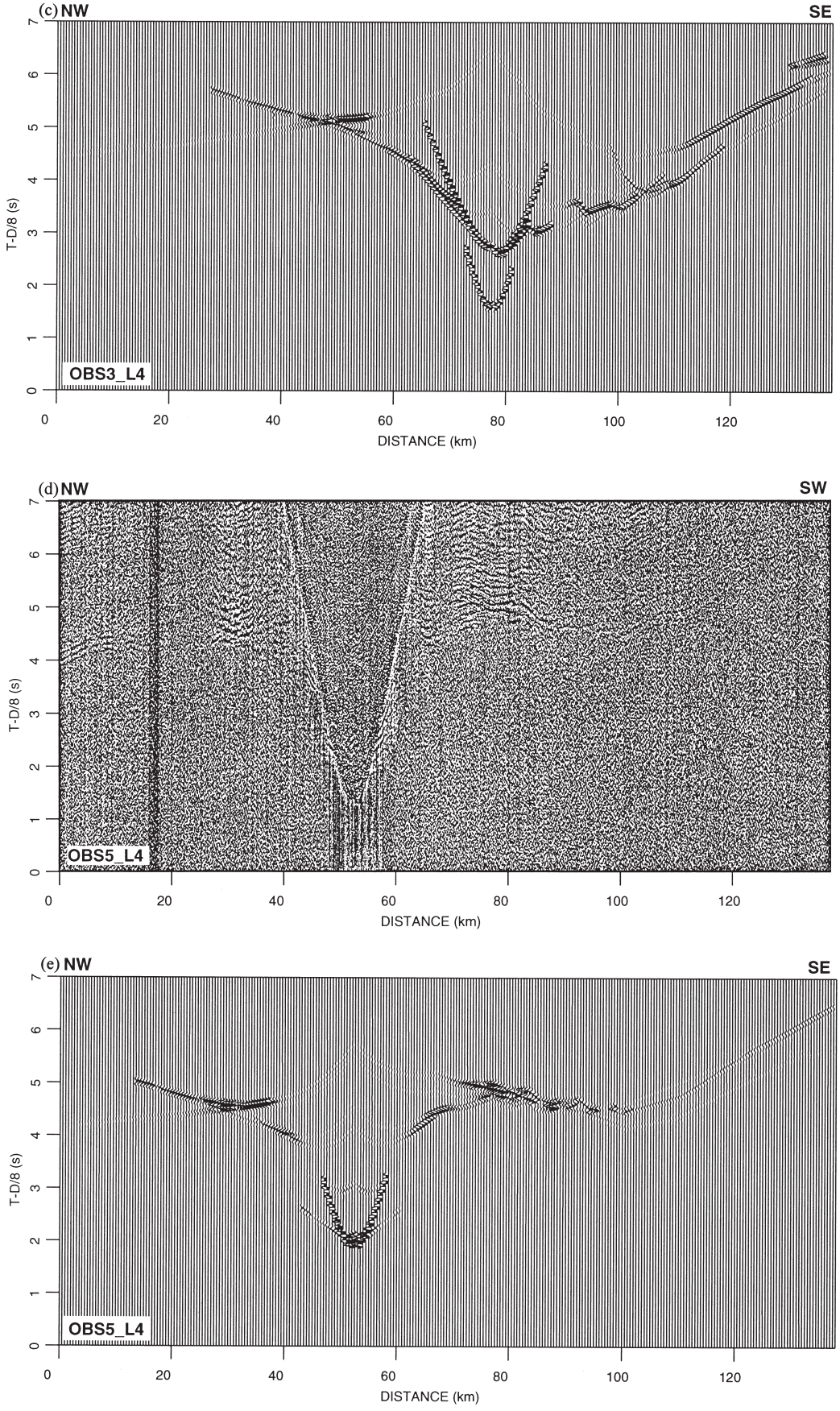

Figure 3. (*Continued.*)

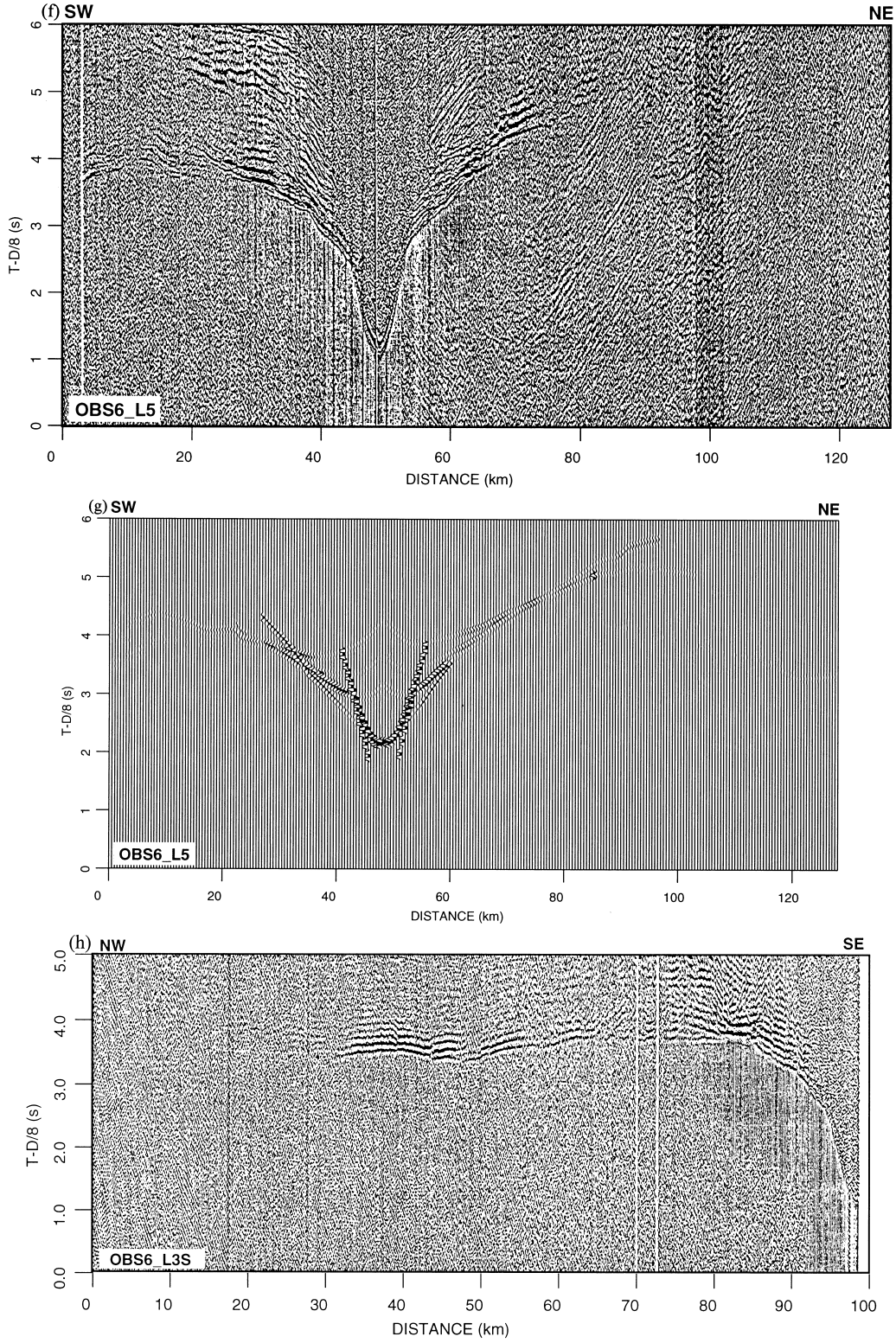

Figure 3. (*Continued.*)

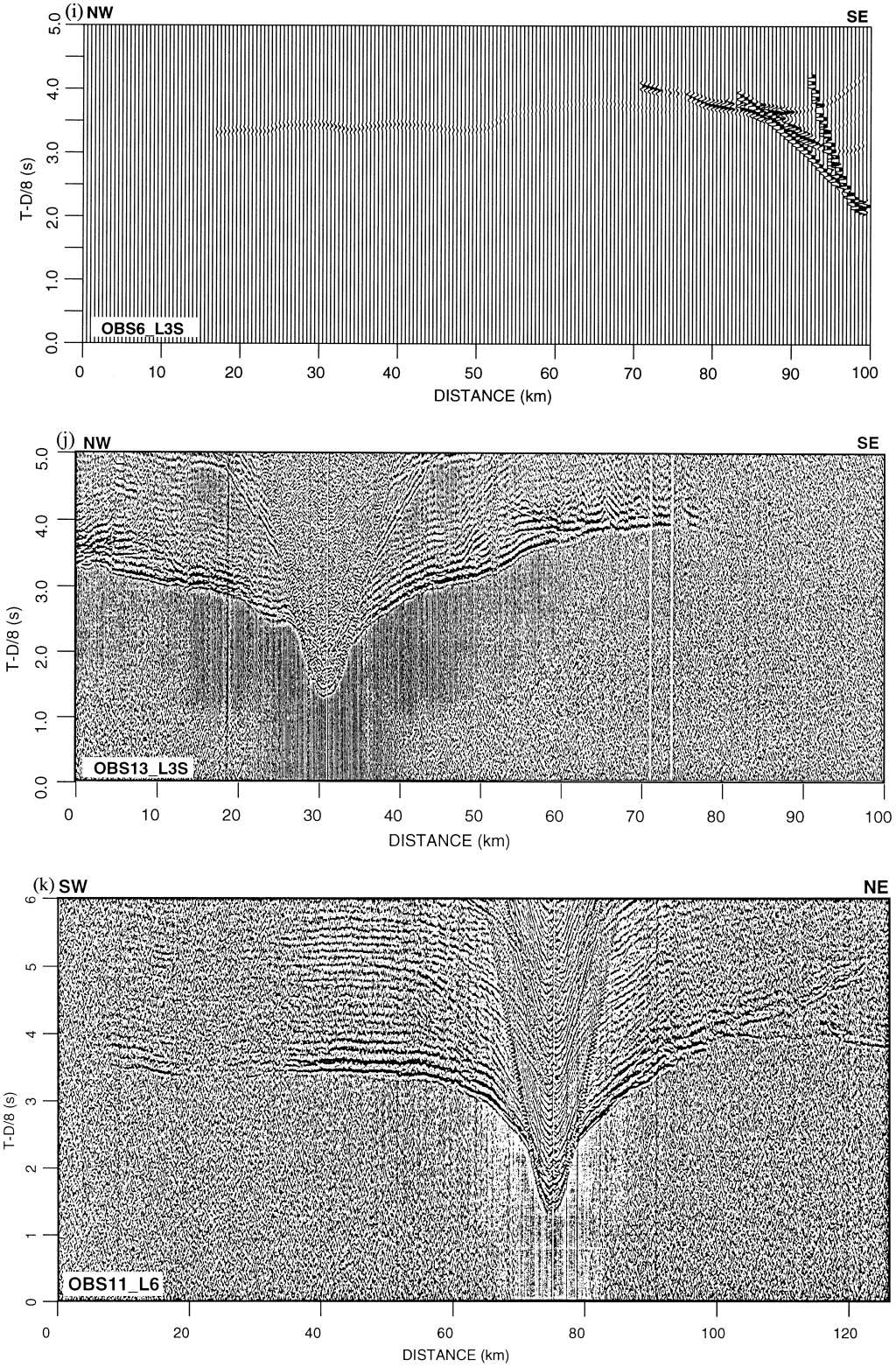

Figure 3. (*Continued.*)

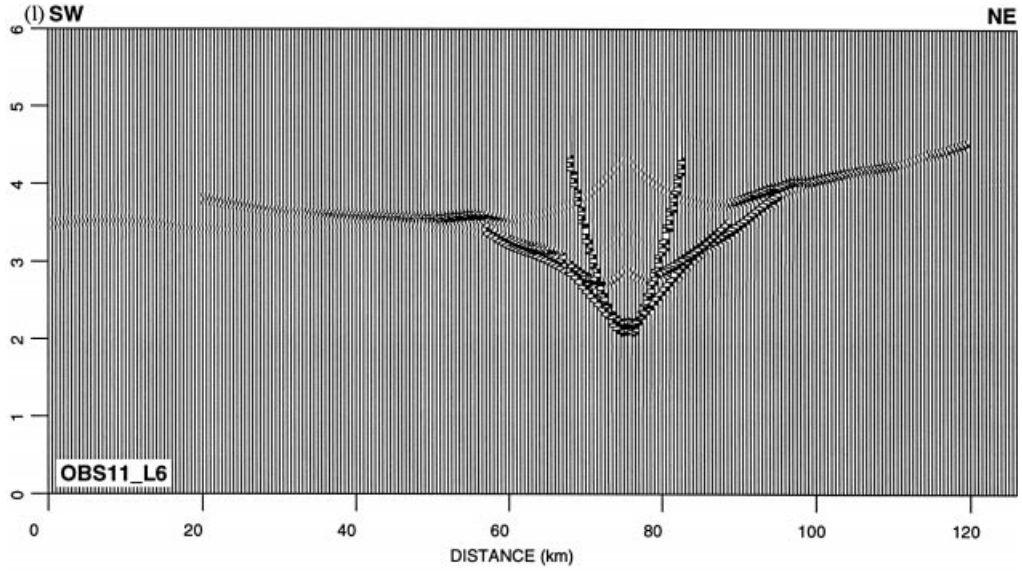

Figure 3. (*Continued.*)

phases at OBS1–3. Clear wide-angle reflection phases from the top of the underplated material would almost certainly have been observed at OBS1–3, as identified along the Norwegian margin (Olafsson *et al.* 1992; Mjelde *et al.* 1997), if high-velocity underplated material were situated beneath the ridge centre. Based on crustal velocity information obtained by a sonobuoy refraction study, Olafsson & Gunnarsson (1989) also suggested that no thick high-velocity layers were present in the lower crust.

From the Jan Mayen Ridge to the Jan Mayen Basin

As shown in Fig. 4, the crustal structure between the Jan Mayen Ridge and the Jan Mayen Basin is characterized by a deep sedimentary basin, a thin basalt layer in the sediments and an extremely thinned continental crust. At the western flank of the Jan Mayen Ridge, geometries down to the top of the 4.0 km s^{-1} layer, dominated by rotated fault blocks, were obtained by interpreting the multichannel reflection data. However, the multichannel data only map the top of the very shallow 4.6–5.0 km s^{-1} layer in the Jan Mayen Basin. Based on interpretations of the reflection data, the sediments above the 4.0 km s^{-1} layer are interpreted as Cenozoic sediments and the 4.0 km s^{-1} layer is interpreted as Mesozoic sediments (Myhre *et al.* 1984). The seismically opaque layer in the Jan Mayen Basin, observed on multichannel reflection data, is interpreted as a basaltic layer erupted at about 30 Ma, and this layer corresponds to our 4.6–5.0 km s^{-1} layer (Kuvaas, personal communication). The thickness of this layer (about 500 m) is uncertain because of velocity inversion beneath it.

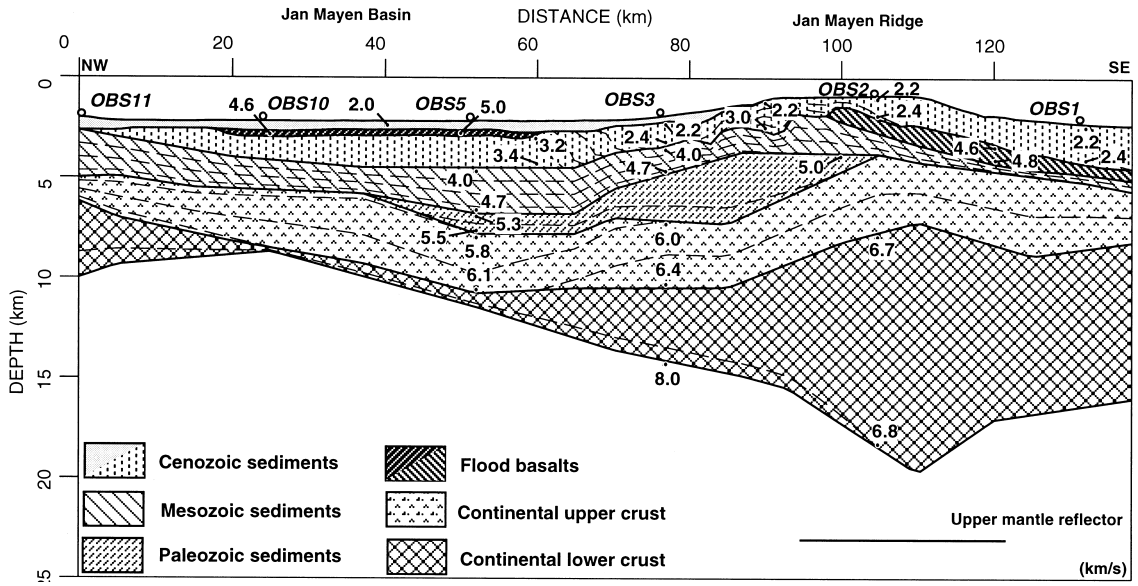

Figure 4. The *P*-wave velocity model of L4 across the Jan Mayen Ridge to the Jan Mayen Basin and its geological interpretation. The horizontal axis indicates the distance from the northwestern end of L4 (Fig. 2). The bold numbers represent *P*-wave velocities (km s^{-1}) at the top and bottom of the layers. The italic numbers represent the OBSs. The isovelocity contour interval is 0.2 km s^{-1}.

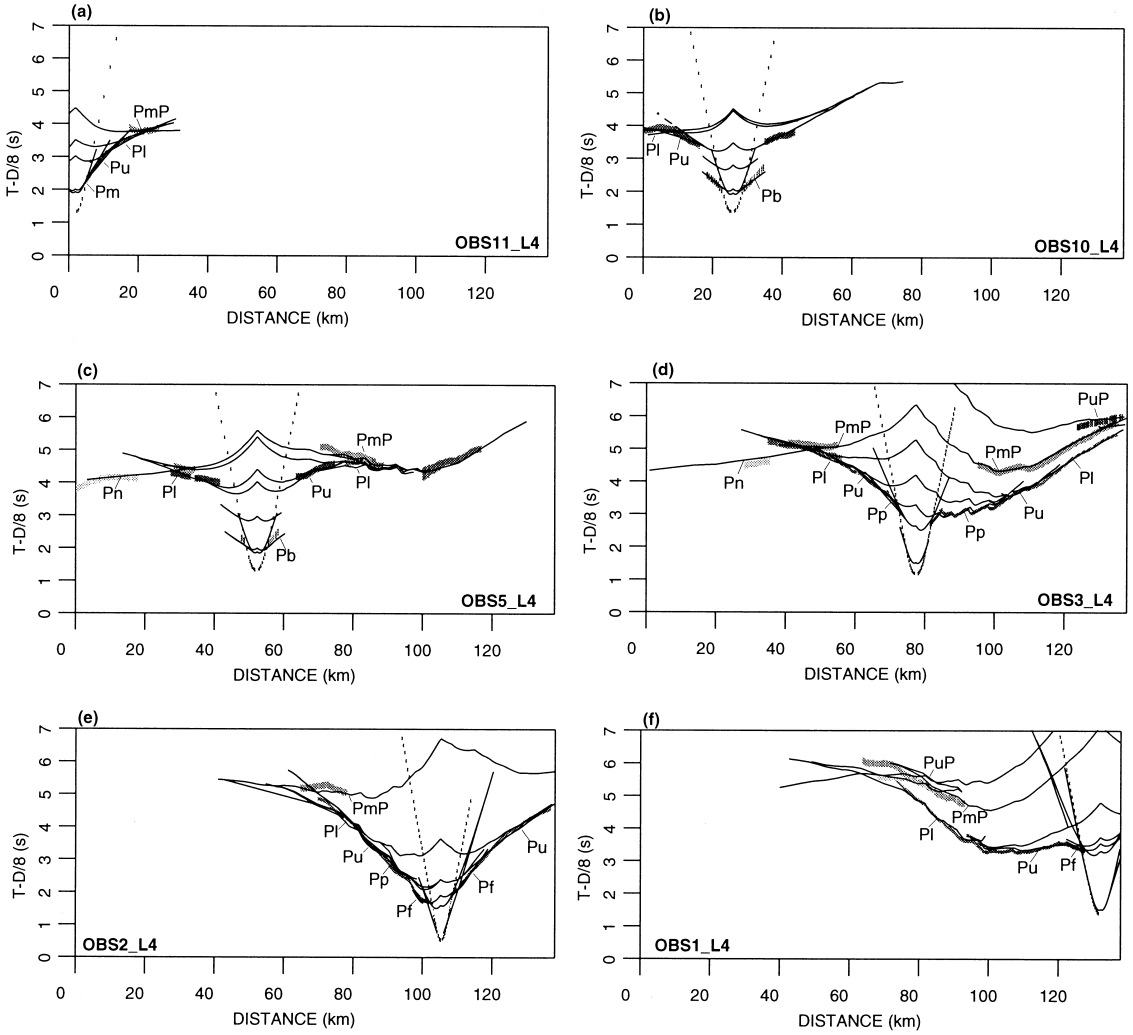

Figure 5. The observed arrivals and calculated traveltime curves of the OBSs on L4. The horizontal axis is the same as in the model of L4. The vertical bars represent uncertainty of observed arrivals varying from 0.05 to 0.2 s. The curved lines represent calculated traveltimes. (a) OBS11. Pm: refraction arrivals from the Mesozoic sediment; Pu: refraction arrivals from the continental upper crust; Pl: refraction arrivals from the continental lower crust; PmP: reflection arrivals from the Moho. (b) OBS10. Pb: refraction arrivals from the basaltic layer beneath the Jan Mayen Basin. (c) OBS5. Pn: refraction arrivals from the uppermost mantle. (d) OBS3. Pp: refraction arrivals from the Palaeozoic sediments; PuP: reflection arrivals from the upper-mantle reflector. (e) OBS2. Pf: refraction arrivals from the flood basalts at the eastern flank of the Jan Mayen Ridge. (f) OBS1.

However, we believe that this is a reliable estimate, since synthetic seismograms explain the gross amplitude variations with offset observed for the refraction phases from this layer (Figs 3d, 3e and Fig. 5c).

Beneath the basaltic layer, the model indicates velocities of 3.2–3.4 km s^{-1} (Cenozoic sediments) and 4.0–4.7 km s^{-1} (Mesozoic sediment) along L4. As shown in the resolution values and ray diagrams (Figs 6a and b), these velocities were not as well resolved as other velocities. However, the same velocities are obtained in the corresponding layer along L5 (Fig. 7), where they are resolved with sufficient accuracy, since the low-velocity layers only exist in the central part of the profile (Figs 7 and 8).

Between the Jan Mayen Ridge and the central part of the Jan Mayen Basin, a layer with a velocity of 5.0–5.5 km s^{-1} (maximum thickness of 3.5 km) is obtained (Fig. 4). The model along L5 indicates that this sedimentary layer does not extend to the southern part of the Jan Mayen Basin. A similar deep sedimentary basin with a velocity of more than 5.5 km s^{-1} has been found at the conjugate eastern Greenland margin (Weigel *et al.* 1995), and the deepest part of that basin is interpreted as Devonian–lower Permian sediments (Surlyk 1991).

Two layers of crystalline crust (V_p = 5.8–6.1 km s^{-1} and 6.7–6.8 km s^{-1}) are present beneath the deep sedimentary basin. These continue from the eastern flank of the Jan Mayen Ridge and are thus interpreted as continental upper and lower crust. The thickness of the continental upper crust (3 km) is generally uniform along L4, but the velocity in this layer is decreased from 6.0 km s^{-1} to 5.8 km s^{-1} towards the Jan Mayen Basin. The crustal model indicates a significant lateral variation in thickness in the continental lower crust. The lower crust becomes thinner towards the Iceland Plateau, and beneath OBS10 it thins to almost zero thickness. As shown in Figs 6(a) and (d), the thinning of the crust is well constrained by Moho reflection and uppermost mantle reflection phases.

In normal continental crust, it is rare to have as high a ratio of lower to upper crust as we observed at the Jan Mayen Ridge (Christensen & Mooney 1995). However, similar high

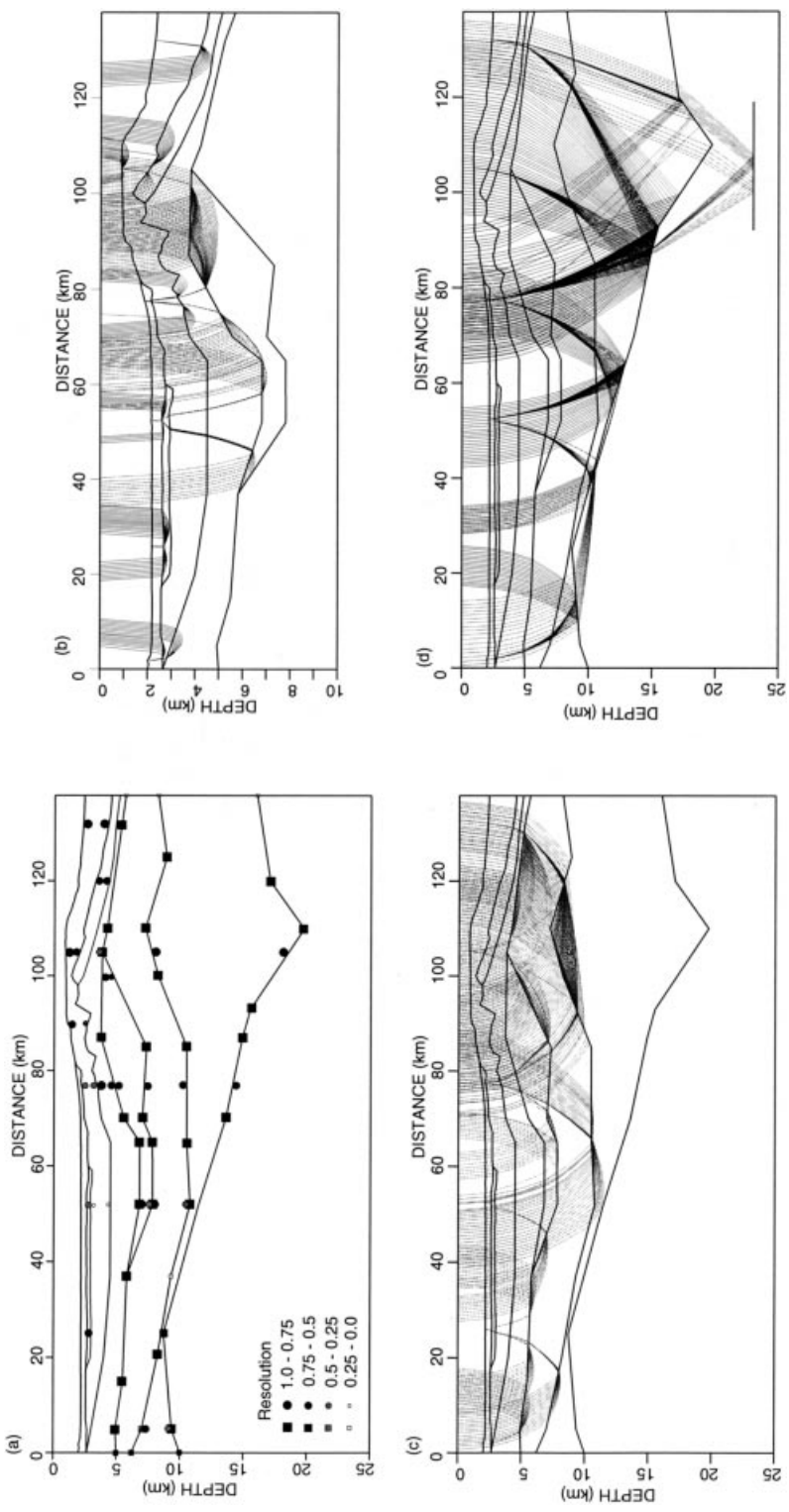

Figure 6. Resolution values and ray diagrams of L4. (a) The resolution values of the velocity nodes (circles) and the interface nodes (squares) for the model. (b) The ray diagram of the sedimentary arrivals. (c) The ray diagram of the refraction arrivals from the upper and lower continental crust. (d) The ray diagram of the reflection arrivals from the Moho and upper-mantle reflector, and uppermost-mantle refraction arrivals.

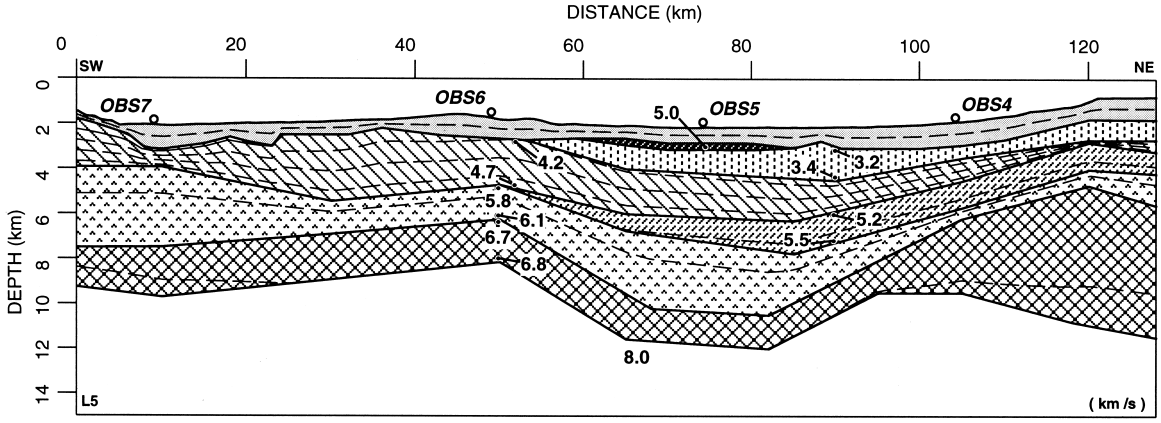

Figure 7. The *P*-wave velocity model of L5 situated at the eastern edge of the Jan Mayen Basin and its geological interpretation. The horizontal axis indicates the distance from the southwestern end of L5 (Fig. 2). The bold numbers represent *P*-wave velocities (km s^{-1}) at the top and bottom of the layers. The italic numbers represent the OBSs. The isovelocity contour interval is 0.2 km s^{-1}.

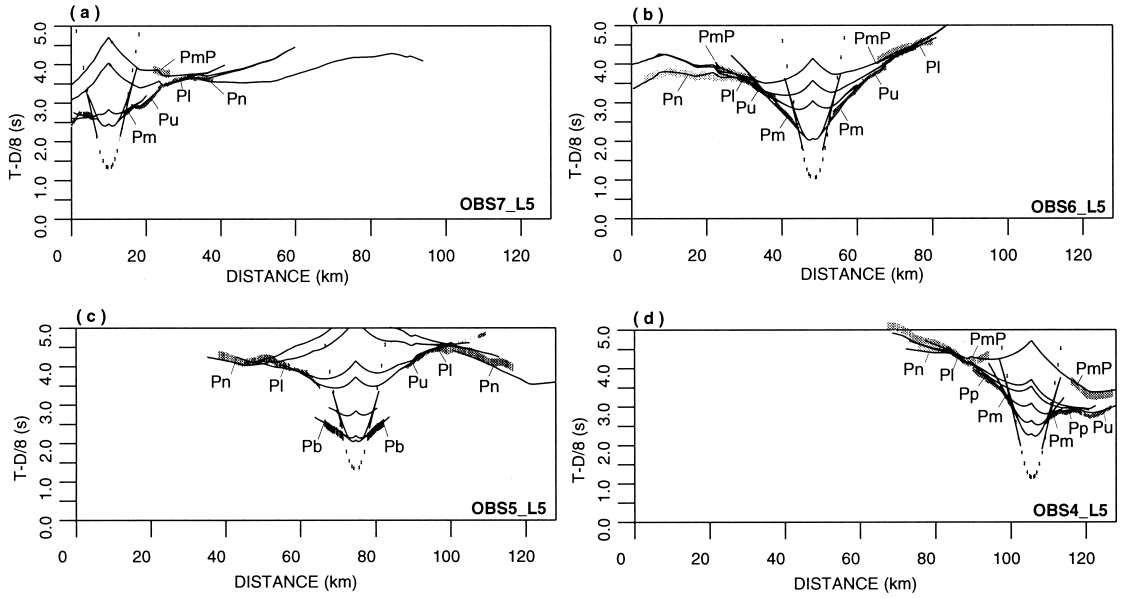

Figure 8. The observed arrivals and calculated traveltime curves of the OBSs on L5. The horizontal axis is the same as in the model of L5. The vertical bars represent uncertainty of observed arrivals varying from 0.05 to 0.2 s. The curved lines represent calculated traveltimes. (a) OBS7. Pm: refraction arrivals from the Mesozoic sediment; Pu: refraction arrivals from the continental upper crust; Pl: refraction arrivals from the continental lower crust; Pn: refraction arrivals from the uppermost mantle; PmP: reflection arrivals from the Moho. (b) OBS6. (c) OBS5. Pb: refraction arrivals from the basaltic layer beneath the Jan Mayen Basin. (d) OBS4. Pp: refraction arrivals from the Palaeozoic sediment.

ratios of lower to upper continental crust are observed at several rifted continental margins. For example, at the eastern Greenland margin, which is the conjugate margin of the Jan Mayen Ridge, a crustal model shows an upper crust (V_p = 6.0–6.6 km s^{-1}) 8–5 km thick accompanying a lower crust (V_p = 6.8–6.9 km s^{-1}) 25–15 km thick (Weigel *et al.* 1995). Moreover, Ruppel (1995) suggested that a high ratio of lower to upper crust might be due to ductile lower-crustal flow derived from an extensional process in continental lithosphere. He also described the extension process giving rise to normal faults in the brittle upper crust. We therefore suggest that the observed velocity reduction in the upper crust beneath the Jan Mayen Basin may be caused by the development of the faults cutting through the upper crust.

From the Jan Mayen Basin to the Iceland Plateau

Fig. 9 shows the crustal model along L3S. The calculated traveltimes for this model are plotted in Fig. 10 with the observed traveltimes. This model is characterized by a transitional structure from the extremely thinned continental crust to a slightly thicker oceanic crust. In the Jan Mayen Basin around OBS6, the model consists of two sedimentary layers (V_p = 2.0 and 4.2–4.7 km s^{-1}) and the upper (V_p = 5.8–6.1 km s^{-1}) and lower continental crust (V_p = 6.7–6.8 km s^{-1}), which corresponds to the structure obtained in the southwestern part of L5 (Fig. 7). As shown in the model, the total thickness of the crystalline crust in this part of the area is estimated at only 3–4 km. This thinned structure is clearly observed in the data

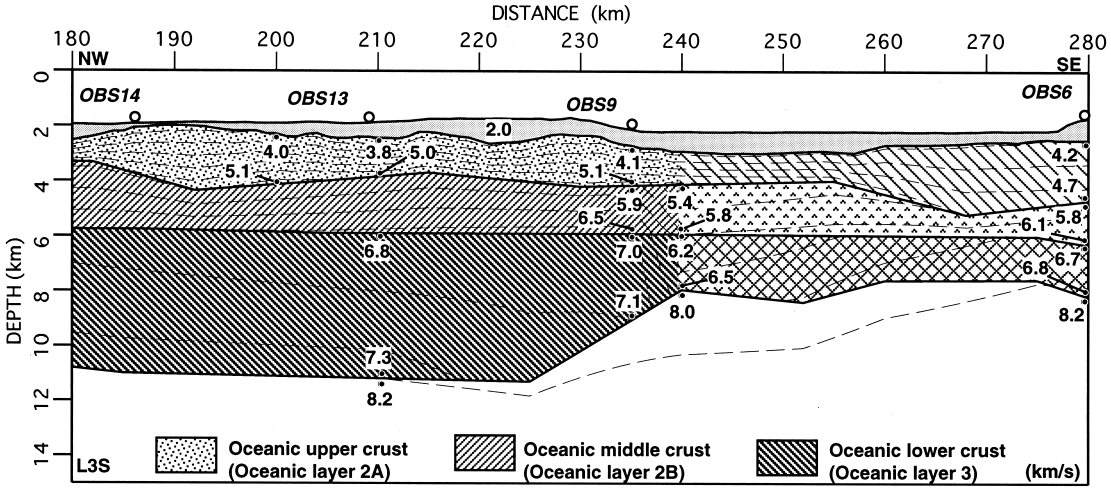

Figure 9. The *P*-wave velocity model of L3S from the Jan Mayen Basin to the Iceland Plateau and its geological interpretation. The horizontal axis indicates the distance from the northwestern end of L3S (Fig. 2). The bold numbers represent *P*-wave velocities (km s^{-1}) at the top and bottom of the layers. The italic numbers represent the OBSs. The isovelocity contour interval is 0.2 km s^{-1}.

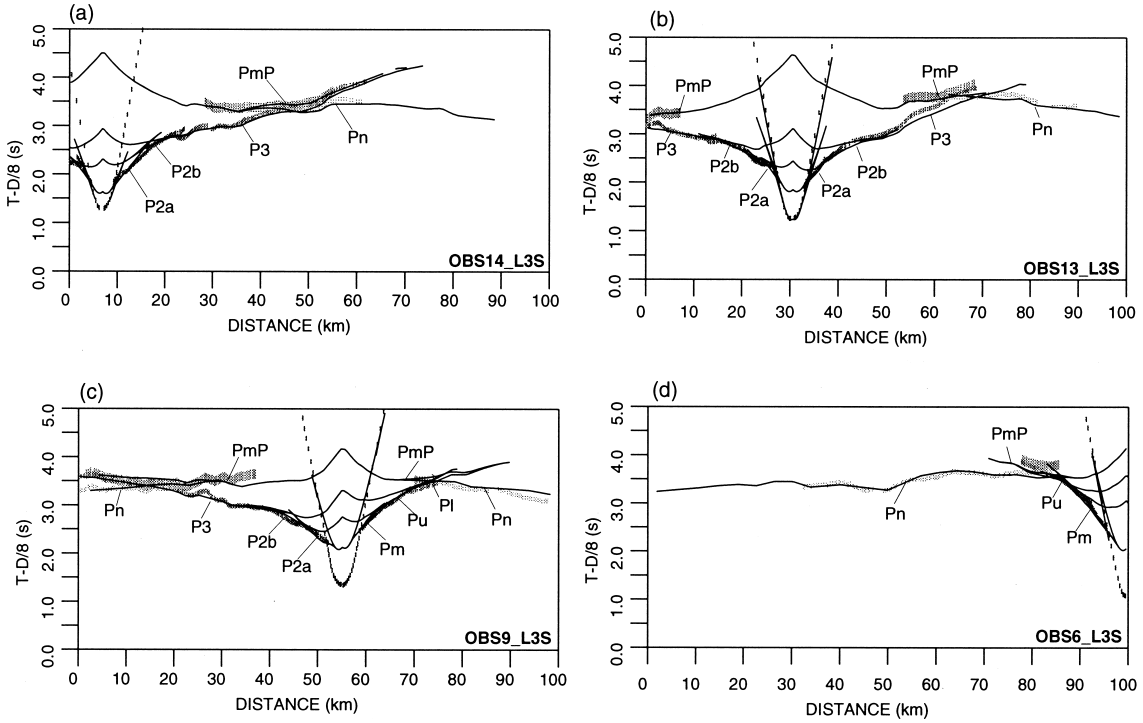

Figure 10. The observed arrivals and calculated traveltime curves of the OBSs on L3S. The horizontal axis is the same as in the model of L3S. The vertical bars represent uncertainty of observed arrivals varying from 0.05 to 0.2 s. The curved lines represent calculated traveltimes. (a) OBS14. P2a: refraction arrivals from the oceanic layer 2A; P2b: refraction arrivals from the oceanic layer 2B; P3: refraction arrivals from the oceanic layer 3; Pn: refraction arrivals from the uppermost mantle; PmP: reflection arrivals from the Moho. (b) OBS13. (c) OBS9. Pm: refraction arrivals from the Mesozoic sediment; Pu: refraction arrivals from the continental upper crust; Pl: refraction arrivals from the continental lower crust. (d) OBS6.

from OBS6 (Fig. 3h), where the mantle refraction arrival is identified as a first arrival at small offsets (12 km). As shown by Bown & White (1995), extreme thinning of continental crust is not unusual, especially at the North Atlantic non-volcanic continental margin. They showed that continental crust thicknesses adjacent to the ocean–continent transition zones vary between 2.1 and 7.6 km; moreover, in half of these cases, the crust is less than 4 km thick with the minimum thickness of 2.1 km at the Iberian margin (Whitmarsh *et al.* 1996).

In the northwestern part of L3S, beneath the sedimentary layer (V_p = 2.0 km s^{-1}), the model consists of three layers (V_p = 3.8–5.1 km s^{-1}, 5.9–6.5 km s^{-1} and 6.8–7.3 km s^{-1}). Vogt *et al.* (1980) identified clear magnetic anomalies in this area, and thus suggested the existence of oceanic crust. Moreover, following the typical oceanic crustal structure compiled

by White (1992), the velocities obtained here for the upper (3.8–5.1 km s^{-1}) and middle crust (5.9–6.5 km s^{-1}) are within the range of typical velocities of oceanic layer 2 (2.5–6.6 km s^{-1}), and the velocities obtained for the lower crust are within the range of typical velocities of oceanic layer 3 (6.6–7.6 km s^{-1}). We have therefore interpreted these three layers as the oceanic crust. In terms of the geological interpretation of the seismically determined oceanic crust (Kent *et al.* 1978), the upper, middle and lower crust obtained in the northwestern part of L3S correspond to pillow lavas (oceanic layer 2A), sheeted dykes (oceanic layer 2B) and the plutonic complex (oceanic layer 3), respectively.

White, McKenzie & O'Nions (1992) found that the oceanic crustal thicknesses are very similar in many areas away from anomalous regions such as fracture zones and hot spots, and they estimated the mean thickness of normal oceanic crust as 7.0 ± 0.8 km. In the northwestern part of the model of L3S, the total thickness of the igneous crust is estimated at about 9 km, which is 2 km thicker than normal oceanic crust. Similar thick oceanic crust has been found in the North Atlantic (Evans & Sacks 1979; White *et al.* 1987; Mutter *et al.* 1988; Fowler *et al.* 1989; Olafsson *et al.* 1992; Mjelde *et al.* 1992; Goldschmidt-Rokita *et al.* 1994; Kodaira *et al.* 1995; Smallwood, White & Minshull 1995). In order to explain these structures, White & McKenzie (1989) applied a model of partial melting by decompression of passively ascending asthenospheric material. They concluded that if the temperature of the ascending material was 100–200 °C higher than normal asthenospheric temperatures, a thick oceanic crust would be created along the spreading axis. They also suggested the Icelandic hot spot as a heat source in the northern Atlantic. Following their study, the thicker oceanic crust identified in the southwestern part of L3S is interpreted as having been generated by the melting of hot asthenosphere as a result of upwelling and decompression under the influence of the Iceland hot spot.

At the western edge of the Jan Mayen Basin, the ocean/continent transition zone is resolved, where crustal velocities increase westwards in a narrow zone only 10 km wide, and approach the velocities of the oceanic crust obtained at the Iceland Plateau (Fig. 9). As shown in Fig. 11, the geometries and velocities at the transition zone are obtained with good resolution (>0.5), except for the velocity in the bottom of the continental upper crust/oceanic layer 2B. Similar velocity variations are obtained along L6 (Fig. 12), where velocities in the two lowermost layers become faster towards the southwest. Calculated traveltimes from this model are shown in Fig. 13. This structure is also interpreted as the ocean/continent transition zone, and the southwestern and northeastern parts of the profile are interpreted as oceanic and continental crust, respectively. Since the models presented do not display any sharp boundary across the ocean/continent transition zone, we believe that the transition structure consists of continental crustal material with intrusions of oceanic crustal material, as proposed by Mjelde *et al.* (1997). The location of this transition zone corresponds to the intersection between L6 and the magnetic quiet zone (Fig. 2). We therefore suggest that the ocean/continent transition zone to the west of the Jan Mayen Ridge is situated along the western edge of the magnetic quiet zone.

Vogt *et al.* (1980) suggested the possible presence of oceanic crust beneath the Jan Mayen Basin. However, the results of the present study do not show any evidence of this. In the top of the continental upper crust along L6, material of a lower velocity (5.4 km s^{-1}) than in the other profiles is present. This might imply that the Palaeozoic sediment (5.0–5.5 km s^{-1}) obtained along L4 exists at the northeastern part of L6. Immediately northwestwards of the transition zone along L3S, the oceanic crust increases in thickness from 5 to 9 km. This structure suggests that immediately after the continental breakup between Jan Mayen and Greenland, very thin oceanic crust was generated.

Along L3S a lateral reduction in mantle velocity from 8.2 to 8.0 km s^{-1} is found beneath the extremely thinned continental crust (Fig. 9). Fig. 11 indicates good seismic ray coverage in this part, and the velocities are estimated with resolution values greater than 0.75. Similar reductions in mantle velocity are obtained beneath thinned continental crust along non-volcanic margins, for example at the Tagus Abyssal Plain (Pinheiro, Whitmarsh & Miles 1992), the southwest Greenland margin (Chian & Louden 1994) and the Iberian margin (Whitmarsh *et al.* 1996).

Implications for the continental rifting to the west of Jan Mayen Ridge

The crustal structures from the west of the Jan Mayen Ridge to the Iceland Plateau (L3S and L4) are summarized as follows: extreme thinning of the continental crust (down to 3 km) within a 100 km wide zone; small amounts of extrusive basalts; no high-velocity underplated material; extremely thin oceanic crust (5 km) immediately westwards of the ocean/continent transition; and thicker oceanic crust (9 km) beneath the Iceland Plateau. Similar structures have been found along the non-volcanic rifted margins of the North Atlantic, for example the Goban Spur (Horsefield *et al.* 1994) and the southwest Greenland margin (Chian & Louden 1994), where the continental crust is characterized by considerable thinning without the emplacement of huge volumes of magmatic material.

In order to explain the crustal structures obtained along the non-volcanic rifted margins, Bown & White (1995) applied a model for melt generation by mantle decompression during uniform pure-shear extension of continental lithosphere at finite rates of rifting. They concluded that melt generation is strongly dependent on rift duration, because most melt is generated in the region near the top of the upwelling asthenosphere, where conductive cooling is greatest

The minimum rifting duration between the Jan Mayen Ridge and Greenland is estimated to be 11–18 Myr, since the oldest magnetic anomaly to the west of the Jan Mayen Basin is anomaly 6 or 7 (Vogt *et al.* 1980) and the youngest magnetic anomaly to the east of the Jan Mayen Ridge is anomaly 13 (Eldholm *et al.* 1990). A geomagnetic timescale obtained by Heirtzler *et al.* (1968) and Cande & Kent (1992) is used in order to convert the magnetic anomaly into the age. It is possible that the duration of rifting was longer than 11–18 Myr, if part of the rifting progressed simultaneously with the oceanic spreading along the Aegir ridge. The stretching factor at the ocean/continent transition is estimated to be about 5, if the crustal thickness beneath the Jan Mayen Ridge is taken as the original thickness of the continental crust before rifting. Referring to White & McKenzie (1989), the crustal thickness of 9 km at the Iceland Plateau implies that the potential

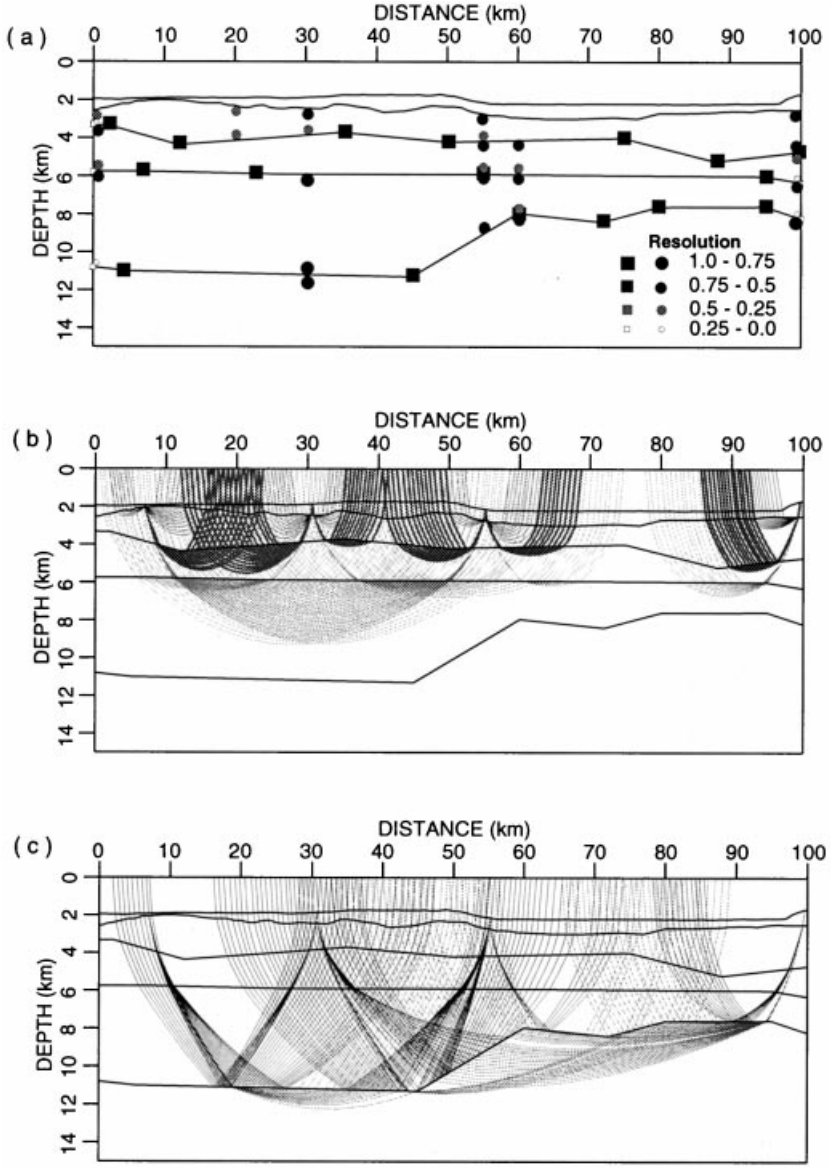

Figure 11. Resolution values and ray diagrams of L3S. (a) The resolution values of the velocity nodes (circles) and the interface nodes (squares) for the model. (b) The ray diagram of the refraction arrivals from the sediment and igneous crust. (c) The ray diagram of the Moho reflection and uppermost mantle refraction arrivals.

temperature of the upwelling material around the Jan Mayen Ridge was about 1320 °C, which is slightly hotter than normal asthenospheric temperatures. In this estimation we have assumed that the potential temperatures did not change during the rifting and oceanic spreading stage. By applying these values to the model by Bown & White (1995), less than 0.5 km thickness of melt is estimated beneath the western part of the Jan Mayen Ridge during rifting. This thickness of melt is in agreement with the crustal structure we obtained, which is characterized by small amounts of extrusive material and no observable high-velocity underplated material beneath the western part of the ridge. The anomalously thin oceanic crust immediately oceanwards of the ocean/continent transition zone also implies that the initially thin oceanic crust was formed from mantle cooled conductively as it upwelled beneath the slowly stretching continental lithosphere.

Following an interpretation by Bown & White (1995), our observed reduction in mantle velocity at the western edge of the Jan Mayen Basin may be the result of partial serpentinization of original mantle material. Where the crust is extremely thin, water may pass through the crust and into the uppermost mantle. This process would cause partial serpentinization of the peridotites, and consequently reduce their seismic velocity (Bown & White 1995).

From the above discussion, although the crust to the east of the Jan Mayen Ridge is considered to be a volcanic continental margin (Skogseid & Eldholm 1987), we propose to refer to the crustal structure to the west of the Jan Mayen Ridge as a non-volcanic continental margin, which was generated by the long duration of rifting, We believe that the upwelling asthenospheric material between the western part of the Jan Mayen Ridge and Greenland was slightly hotter than

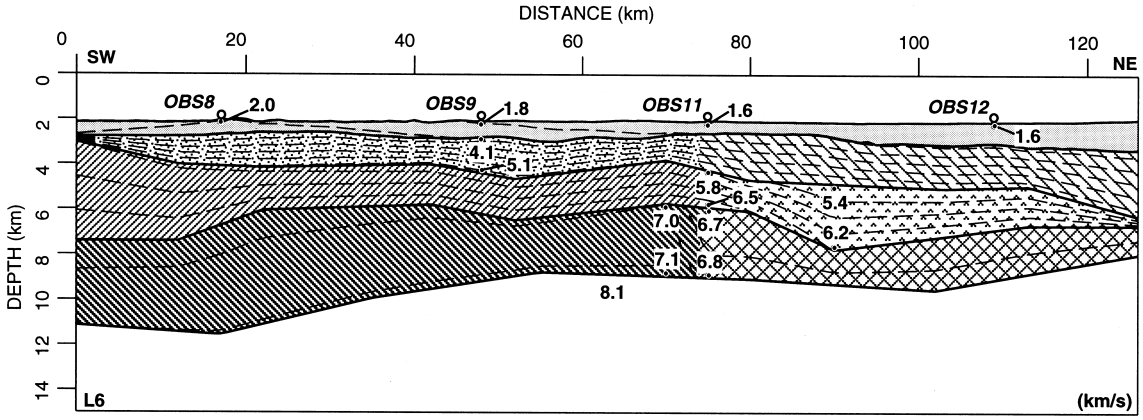

Figure 12. The *P*-wave velocity model of L6 situated at the western edge of the Jan Mayen Basin and its geological interpretation. The horizontal axis indicates the distance from the southwestern end of L6 (Fig. 2). The bold numbers represent *P*-wave velocities (km s^{-1}) at the top and bottom of the layers. The italic numbers represent the OBSs. The isovelocity contour interval is 0.2 km s^{-1}.

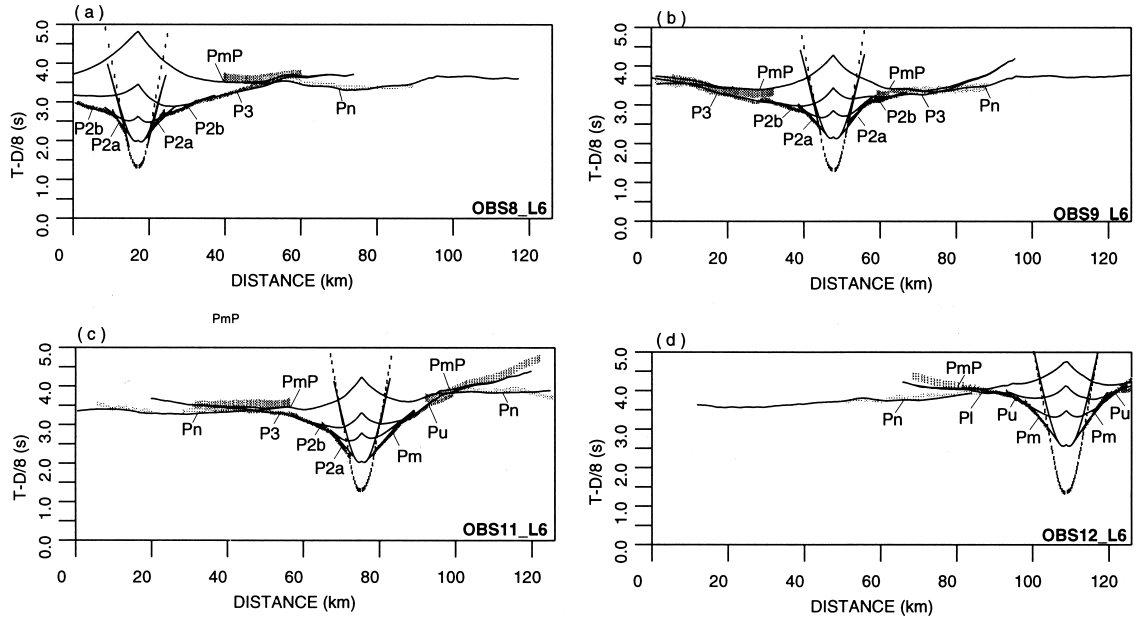

Figure 13. The observed arrivals and calculated traveltime curves of the OBSs on L6. The horizontal axis is the same as in the model of L6. The vertical bars represent uncertainty of observed arrivals varying from 0.05 to 0.2 s. The curved lines represent calculated traveltimes. (a) OBS8. P2a: refraction arrivals from the oceanic layer 2A; P2b: refraction arrivals from the oceanic layer 2B; P3: refraction arrivals from the oceanic layer 3; Pn: refraction arrivals from the uppermost mantle; PmP: reflection arrivals from the Moho. (b) OBS9. (c) OBS11. Pm: refraction arrivals from the Mesozoic sediment; Pu: refraction arrivals from the continental upper crust. (d) OBS12. Pl: refraction arrivals from the continental lower crust.

normal during continental rifting and oceanic spreading, probably due to the influence of the Iceland hot spot, as suggested by White & McKenzie (1989). However, because of the long duration of rifting, conductive heat loss from the upwelling material occurred, and consequently only small amounts of extrusive and intrusive material were generated.

CONCLUSIONS

This paper has presented a model of the crustal structure from the Jan Mayen Ridge to the Iceland Plateau across the Jan Mayen Basin obtained by modelling OBS data. The crustal structures at the eastern flank of the Jan Mayen Ridge are characterized by a flood basalt within the sediments and 11–15 km thick continental crust. The model indicates velocities of 6.0–6.4 km s^{-1} and 6.7–6.8 km s^{-1} in the upper and lower crust, respectively. These velocities show good correspondence with velocities obtained at the conjugate Norwegian margin. Beneath the centre of the Jan Mayen Ridge, however, the crustal model does not show any evidence of the high-velocity underplated materials that have been observed along the conjugate Norwegian margin. Due to a poor coverage of seismic rays to the east of the Jan Mayen Ridge, it might be possible to accept a model incorporating a high-velocity material to the east of the Jan Mayen Ridge. However, even if the high-velocity material exists to the east of the Jan Mayen Ridge, the OBS data strongly suggest that any high-velocity lower-crustal material cannot extend beneath OBS2, which is located at the top of the Jan Mayen Ridge.

From the western flank of the Jan Mayen Ridge to the Jan

Mayen Basin, which is considered to be the conjugate margin of Greenland, the modelling indicates the presence of a deep sedimentary basin (up to 5 km thick), a thin basaltic layer (4.6–5.0 km s^{-1}) in the sediments and two layers of extremely thinned continental crust (5.8–6.1 km s^{-1} and 6.7–6.8 km s^{-1}). The continental upper crust (5.8–6.1 km s^{-1}) shows a uniform thickness (3 km thick) from the Jan Mayen Ridge to the western end of the Jan Mayen Basin. However, the thickness of the continental lower crust (6.7–6.8 km s^{-1}) decreases significantly down to almost zero thickness towards the western part of the Jan Mayen Basin. Consequently, the model indicates that the continental crust to the west of the Jan Mayen Ridge has been thinned to 3 km thickness with restricted magmatic activity during the continental rifting process. Similar structures (that is extreme thinning of continental crust incorporating a high ratio of lower to upper continental crust) are observed at several non-volcanic continental margins. Those structures might be caused by ductile lower-crustal flow derived from an extensional process in continental lithosphere.

At the western edge of the Jan Mayen Basin, we found an ocean/continent transition structure along the magnetic quiet zone, where the *P*-wave velocities approach those obtained at the Iceland Plateau (3.8–5.1 km s^{-1}, 5.9–6.5 km s^{-1} and 6.8–7.3 km s^{-1}). We emphasize that the thickness of the oceanic crust immediately oceanwards of the transition is extremely thin (5 km). The oceanic crust beneath the Iceland Plateau is, however, slightly thicker (9 km) than the typical thickness of normal oceanic crust (7 km).

From the crustal structure presented in this study, we conclude that the area to the west of the Jan Mayen Ridge is a non-volcanic continental margin, associated with a long duration of rifting. We also believe that the passively upwelling material to the west of the Jan Mayen Ridge was slightly hotter than normal, due to the influence of the Iceland hot spot. However, because of the long duration of the rifting, conductive heat loss from the upwelling materials occurred, and consequently small amounts of extrusive and intrusive material were generated.

ACKNOWLEDGMENTS

We thank the crew of R/V Håkon Mosby and all participants of the OBS survey, especially the technical staff and students from the Institute of Solid Earth Physics (IFJ), University of Bergen, and the Laboratory for Ocean Bottom Seismology (LOBS), Hokkaido University. J. P. Fjellanger (IFJ) and A. Nakanishi (LOBS) are greatly acknowledged for their support during the planning and preparation of the experiment. B. Nyland, N. Sørenes and M. Sand of the Norwegian Petroleum Directorate are acknowledged for assisting in the planning of the experiment and for providing essential multichannel reflection data. We acknowledge Icelandic and Norwegian authorities for providing the necessary permission for the survey. Finally, we thank M. A. Sellevoll, P. Digranes and B. Kuvaas (IFJ) for their encouragement, support and comments on the manuscript. Part of the survey was funded by the Ministry of Education, Science and Culture of Japan, and SK was supported by a fellowship from the Norwegian Research Council.

REFERENCES

Bown, J.W. & White, R.S., 1995. Effect of finite extension rate of melt generation at rifted continental margins, *J. geophys. Res.,* **100,** 18 011–18 029.

Cande, S. & Kent, D., 1992. A new geomagnetic polarity time scale for the Late Cretaceous and Cenozoic, *J. geophys. Res.,* **97,** 13 917–13 951.

Červený, V., Molokkov, I. & Pšenčík, I., 1977. *Ray Method in Seismology,* Charles University of Press, Prague, Czech Republic.

Chian, D. & Louden, K.E., 1994. The continent-ocean crustal transition across the southwest Greenland margin, *J. geophys. Res.,* **99,** 9117–9136.

Christensen, N.I. & Mooney, W.D., 1995. Seismic velocity structure and composition of the continental crust: a global view, *J. geophys. Res.,* **100,** 9761–9788.

Eldholm, O. & Windisch, C.C., 1974. Sediment distribution in the Norwegian Greenland Sea, *Geol. Soc. Am. Bull.,* **85,** 1661–1676.

Eldholm, O., Skogseid, J., Sundvor, E. & Myhre A.M., 1990. The Norwegian Greenland Sea, in *The Geology of North America, L: The Arctic Ocean Region,* pp. 351–363, eds Grantz, A., Johnson, L. & Seeney, J.F., Geol. Soc. Am., Boulder, CO.

Evans, J.R. & Sacks, I.S., 1979. Deep structure of the Iceland Plateau, *J. geophys. Res.,* **84,** 6859–6866.

Fowler, S.R., White, R.S., Westbrook, G.K. & Spence, G.D., 1989. The Hatton Bank continental margin—II. Deep structure from two-ship expanding spread seismic profiles, *Geophys. J. Int.,* **96,** 295–309.

Gairaud, H., Jacquart, G., Aubertin, F. & Beuzart., P., 1978. The Jan Mayen Ridge synthesis of geological knowledge and new data, *Oceanologica Acta,* **1,** 335–358.

Garde, S.S., 1978. Zur geologischen Entwicklung des Jan Mayen Ruckens nach geophysikalischen Daten, *Dissertation,* University of Clausthal, Germany.

Goldschmidt-Rokita, A., Hansch, K.J.F., Hirschleber, H.B., Iwasaki, T., Kanazawa, T., Sellevoll, M.A. & Shimamura, H., 1994. The ocean/continental transition along a profile through the Lofoten Basin, Northern Norway, *Mar. geophys. Res.,* **16,** 201–224.

Grønlie, G., Chapman, M. & Talwani, M., 1979. Jan Mayen Ridge and Iceland Plateau: origin and evolution, *Nor. Polarinst. Skr.,* **170,** 25–48.

Grønlie, G. & Talwani, M., 1982. The free-air gravity field of the Norwegian Greenland Sea and adjacent areas, *Earth Evol. Ser.,* **2,** 79–103.

Gudlaugsson, S.T., Gunnarsson, K., Sand, M. & Skogseid, J., 1988. Tectonic and volcanic events at the Jan Mayen Ridge microcontinent, in *Early Tertiary volcanism and the opening of the NE Atlantic,* eds Morton, A.C. & Parson, L.M., *Geol. Soc. Spec. Publ.*, **39,** 85–93.

Heirtzler, J.R., Dickson, G.O., Herron, E.M., Pitman, W.C., III & Le Pichon, X., 1968. Marine magnetic anomalies, geomagnetic field reversals, and motions of the ocean floor and continents, *J. geophys. Res.,* **73,** 2119–2136.

Horsefield, S.J., Whitmarsh, R.B., White, R.S. & Sibuet, J.C., 1994. Crustal structure of the Goban Spur passive continental margin, North Atlantic results form a detailed seismic refraction survey, *Geophys. J. Int.,* **119,** 1–19.

Johansen, B., Ledholm, O., Talwani, M., Stoffa, P.L. & Buhl, P., 1988. Expanding spread profile at the northern Jan Mayen Ridge, *Polar Res.,* **6,** 95–104.

Kanazawa, T., 1986. A seven component, a low power consumption and an acoustic comandable ocean bottom seismograph, *Prog. Abstr. Seism. Soc. Japan,* **2,** 240 (in Japanese).

Kanazawa, T. & Shiobara, H., 1994. Newly developed ocean bottom seismometer, *Prog. Abstr. Japan Earth planet. Sci. Joint Meeting,* 341 (in Japanese).

Kent, D.V., Honnorez, B.M., Opdyke, N.D. & Fox, P.J., 1978. Magnetic properties dredged oceanic gabbros and the source of marine magnetic anomalies, *Geophys. J. R. astr. Soc.,* **55,** 513–537.

Kodaira, S. *et al.*, 1995. Crustal structure of the Lofoten continental

margin, off N. Norway, from ocean bottom seismographic studies, *Geophys. J. Int.,* **121,** 907–924.

McKenzie, D. & Bickle, M.J., 1988. The volume and composition of melt generated by extension of the lithosphere, *J. Petrol.,* **29,** 625–679.

Mjelde, R., Sellevoll, M.A., Shimamura, H., Iwasaki, T. & Kanazawa, T., 1992. A crustal study off Lofoten, N. Norway, by use of 3-component Ocean Bottom Seismographs, *Tectonophysics,* **212,** 269–288.

Mjelde, R., Sellevoll, M.A., Shimamura, H., Iwasaki, T. & Kanazawa, T., 1993. Crustal structure beneath Lofoten, N. Norway, from vertical incidence and wide-angle seismic data, *Geophys. J. Int.,* **114,** 116–126.

Mjelde, R., Kodaira, S. & Shimamura, H., 1995. OBS experiment Kolbeinsey ridge—Jan Mayen ridge, 2–21 May 1995, *Cruise Report,* Inst. Solid Earth Phys., University of Bergen.

Mjelde, R., Kodaira, S., Shimamura, H., Kanazawa, T., Shiobara, H., Berg, E.W. & Riise, O., 1997. Crustal structure of the central part of the Vøring Basin, N. Norway, from three-component Ocean Bottom Seismographs, *Tectonophysics,* **277,** 235–257.

Mutter, J.C., Buck, W.R. & Zehnder, C.M., 1988. Convective partial melting, I, A model for the formation of thick basaltic sequences during the initiation of spreading, *J. geophys. Res.,* **93,** 1031–1048.

Myhre, A.M., 1984. Compilation of seismic velocity measurements along the margins of the Norwegian-Greenland Sea, *Nor. Polarinst. Skr.,* **180,** 46–67.

Myhre, A.M. & Eldholm, O., 1981. Sedimentary and crustal velocities in the Norwegian-Greenland Sea, *J. geophys. Res.,* **86,** 5012–5022.

Myhre, A.M., Eldholm, O. & Sundvor, E., 1984. The Jan Mayen Ridge: present status, *Nor. Polarinst. Skr.,* **2,** 47–59.

Navrestad, T. & Jørgensen, F., 1979. Aeromagnetic investigations on the Jan Mayen Ridge, *Nor. Petrol Soc.,* **NSS9**.

Olafsson, I., 1983. The Jan Mayen Ridge and surrounding areas—a marine geophysical study, *Cand. real. thesi.,* University of Bergen.

Olafsson, I. & Gunnarsson, K., 1989. The Jan Mayen Ridge: velocity structure from analysis of sonobuoy data, *Internal Rept,* National Energy Authority of Iceland.

Olafsson, I., Sundvor, E., Eldholm, O. & Grue, K., 1992. Møre margin: crustal structure from analysis of expanded spread profiles, *Mar. geophys. Res.,* **14,** 137–163.

Pinheiro, L.M., Whitmarsh, R.B. & Miles, P.R., 1992. The ocean-continent boundary off the western continental margin of Iberia—II. Crustal structure in the Tagus Abyssal Plain, *Geophys. J. Int.,* **109,** 106–124.

Ruppel, C., 1995. Extensional processes in continental lithosphere, *J. geophys. Res.,* **100,** 24 187–24 215.

Shimamura, H., 1988. OBS technical description, in *Seismiske Undersøkelser av Lofoten Marginen og Refleksjonsseismiske Test-Målinger på Mohns Rygg,* M/S Håkon Mosby, 29 juli–19 august, 1988, ed. Sellevoll, M.A., *Cruise report,* Inst. Solid Earth Physics, University of Bergen.

Skogseid, J. & Eldholm, O., 1987. Early Cenozoic crust at the Norwegian continental margin and the conjugate Jan Mayen Ridge, *J. geophys. Res.,* **92,** 11 471–11 491.

Smallwood, J.R., White, R.S. & Minshull, T.M., 1995. Sea-floor spreading in the presence of the Iceland plume: the structure of the Reykjanes Ridge at 61°40'N, *J. geol. Soc. Lond.,* **52,** 1023–1029.

Stoffa, P.L. & Buhl, P., 1979. Two-ship multichannel seismic experiments for deep crustal studies, *J. geophys. Res.,* **84,** 7645–7660.

Sundvor, E., Gidskehaug, A., Myhre, A.M. & Eldholm, O., 1979. Marine geophysical survey on the northern Jan Mayen Ridge, Seismol. Observation University of Bergen, *Sci. Rept.,* **6**.

Surlyk, F., 1991. Sequence stratigraphy of the Jurassic-Lowermost Cretaceous of East Greenland, *Am. Assoc. Petrol. Geol. Bull.,* **75,** 1468–1488.

Talwani, M. & Eldholm, O., 1977. Evolution of the Norwegian-Greenland Sea, *Geol. Soc. Am. Bull.,* **88,** 969–999.

Talwani, M. & Grønlie, G., 1976. A free-air map of the Norwegian Sea, *Geol. Soc. Am.,* **MC–15**.

Talwani, M. & Udintsev, G., 1976. Tectonic synthesis, *Init. Rept Deep Sea Drilling Project,* **38,** 1213–1242.

Talwani, M., Udintsev, G., Mirlin, E., Beresnev, A.F., Kanayev, V.F., Chapman, M., Grønlie, G. & Eldholm, O., 1978. Survey sites 236, 347, 348, 349 and 350. The area of the Jan Mayen Ridge and the Icelandic Plateau, *Init. Rept Deep Sea Drilling Project,* **38,** 456–488.

Udintsev, G.B. & Kharin, G.S., 1978. Sedimentary rocks of the Jan Mayen Ridge, *Init. Rept Deep Sea Drilling Project,* **38,** 95–100.

Vogt., P.R., Johnson, G.L. & Kristjansson, L., 1980. Morphology and magnetic anomalies north of Iceland, *J. Geophys.,* **47,** 67–80.

Weigel, W. *et al*., 1995. Investigation of the East Greenland Continental Margin between 70° and 72°N by deep seismic sounding and gravity studies, *Mar. geophys. Res.,* **17,** 167–199.

White, R.S., 1992. Crustal structure and magmatism of North Atlantic continental margins, *J. Geol. Soc. Lond.,* **149,** 841–854.

White, R.S. *et al*., 1987. Hatton Bank (northwest U.K.) continental margin structure, *Geophys. J. R. astr. Soc.,* **89,** 265–272.

White, R.S. & McKenzie, D., 1989. Magmatism at rift zones: the generation of volcanic continental margins and flood basalts, *J. geophys. Res.,* **94,** 7685–7729.

White, R.S., McKenzie, D. & O'Nions, R.K., 1992. Oceanic crustal thickness from seismic measurements and rare earth element inversions, *J. geophys. Res.,* **97,** 19 683–19 715.

Whitmarsh, R.B., White, R.S., Horsefield, S.J., Sibuet, J.-C., Recq, M. & Louvel, V., 1996. The ocean-continent boundary off the western continental margin of Iberia: crustal structure west of Galicia Bank, *J. geophys. Res.,* **101,** 28 291–28 314.

Zelt, C. A & Ellis, R.M., 1988. Practical and efficient ray tracing in two dimensional media for rapid travel-time and amplitude forward modelling, *Can, J. expl. Geophys.,* **24,** 16–31.

Zelt, C.A. & Smith, R.B., 1992. Seismic traveltime inversion for 2-D crustal velocity structure, *Geophys. J. Int.,* **108,** 16–34.